Biological and Medical Applications of Materials and Interfaces

Plasmonic interface modified with graphene oxide sheets overlayer for sensitivity enhancement

Xin Xiong, Yaofei Chen, Hao Wang, Shiqi Hu, Yunhan Luo, Jiangli Dong, Wenguo Zhu, Wentao Qiu, Heyuan Guan, Huihui Lu, Jianhui Yu, Jun Zhang, and Zhe Chen

ACS Appl. Mater. Interfaces, **Just Accepted Manuscript** • DOI: 10.1021/acsami.8b11424 • Publication Date (Web): 20 Sep 2018

Plasmonic interface modified with graphene oxide sheets overlayer for sensitivity enhancement

Xin Xiong,[1,4] Yaofei Chen,[2,3,4] Hao Wang,[1] Shiqi Hu,[1] Yunhan Luo,[1,2,] Jiangli Dong,[2,3] Wenguo Zhu,[2,3] Wentao Qiu,[2,3] Heyuan Guan,[1,2] Huihui Lu,[1,3] Jianhui Yu,[1,3] Jun Zhang,[3] Zhe Chen[2,3]*

[1]Guangdong Provincial Key Laboratory of Optical Fiber Sensing and Communications, Jinan University, Guangzhou 510632, China

[2]Key Laboratory of Optoelectronic Information and Sensing Technologies of Guangdong Higher Education Institutes, Jinan University, Guangzhou 510632, China

[3]Key Laboratory of Visible Light Communications of Guangzhou, Jinan University, Guangzhou 510632, China

[4]The equivalent contributors to this work

*Corresponding author: luoyunhan@jnu.edu.cn

ABSTRACT: A novel strategy to modify the plasmonic interface by spin-coating an overlayer of graphene oxide sheets (GOSs) on the top of the surface plasmon sensor (SPR) is proposed and demonstrated. Thanks to the excellent electrical conductivity, large surface area and high refractive index of the GOSs layer, the GOSs modified SPR (GOSs-SPR) sensor achieves an improved sensitivity in the detection of bulky refractive index solutions and bovine serum albumin (BSA) solutions. More importantly, the sensitivity of the GOSs-SPR sensor can be

tuned via changing the thickness of the GOSs overlayer, which in turn can be tailored by spin-coating GOSs ethanol suspension for different times. The maximum sensitivity of 2715.1 nm/RIU achieved by three times spin-coating shows an enhancement of 20.2% than the case without modification of GOSs overlayer. Benefiting from the large surface area and abundant surface functional groups, the GOSs-SPR sensor has a greater sensitivity enhancement (up to 39.35%) in the detection of the BSA molecules. Additionally, the proposed modification method for the plasmonic interface is a simple and effective strategy to boost the sensitivity in a chemical-free and environment-friendly manner, without additional chemical or biological amplification steps. These unique features make the proposed GOSs-SPR biosensor a low-cost and biocompatible platform in the fields of biochemical sensing, drug screening, and environmental monitoring.

KEYWORDS: Plasmonic interface, graphene oxide sheets, sensitivity enhancement, refractive index, bovine serum albumin

INTRODUCTION

The rapid development of various functionalized materials and interfaces for analysing molecular interactions has been driven over the last two decades by the increasing demand for a better understanding of the specific interactions among biomolecules, which provides insights into fundamental biological processes and serve as the cornerstones of life science research and medical diagnosis.[1] Plasmonic interface has attracted great attention because of its advantages such as highly sensitive, label-free, and real-time detection manner for bimolecular interactions and chemical analytes.[2-5] Although the surface plasmon resonance (SPR)technologies have been widely investigated in the field of life science, food quality assurance, and drug screening, they are still facing challenges in the detection of small molecular with molecules weight less than

500 Da and ultralow concentration of analytes.[6-8] To overcome this limitation, a number of plasmonic interfaces have been proposed to enhance the sensitivity of SPR sensors,[9] for example, combining the strong electric field of localized SPR excitation based on metal nanoparticles,[10-12] utilizing a complex nanostructure between the substrate and analyte instead of a common metal film,[13-15] exciting long-range surface plasmon to achieve a ultrahigh penetration depth,[16-17] or depositing on the metal film with an additional layer of high refractive index (RI) materials such as Si, Al_2O_3, ITO and ZnO.[18-20] However, these methods usually have a demand of chemical synthesizing or manufacturing in nanoscale, which would be limited in wide application. Recently, a simple and effective method to enhance sensitivity of SPR sensors by depositing a nanomaterial overlayer, e.g. halloysite nano-tubes (HNTs), tungsten disulphide (WS_2), TiO_2, graphene and $MoSe_2$,[21-24] on the surface of metal film has been demonstrated. The advantage for the interface modification method with overlayer deposition is easy to operate and flexible to change the thickness. Moreover, the large specific surface area provides large number of accommodation for bimolecular, which is beneficial to the detection of molecules with low weight or concentration.

Graphene, which consists of a one-atom-thick planar sheet comprising a sp^2-bonded carbons structure with exceptionally high crystal and electronic quality, has received significant interest in the past few years due to its outstanding properties including extraordinary mechanical strength, prominent electrical conductivity, facile surface modification, large surface area, and good biocompatibility.[25-27] These properties make graphene a promising material in the field of SPR biosensors.[28-29] Functionalized graphene sheets, also called graphene oxide sheets (GOSs), are the oxidized counterparts of graphene and have many remarkable properties, owing to their ability in adsorbing oxygen onto their surface in the form of epoxy (-O), hydroxyl (-OH), and

carboxyl (-COOH). The controlled adsorption of oxygen onto graphene can increase its optical band gap and allow its propagation constant of the surface plasmon polariton to be modified, thus its optical properties to be manipulated.[30-32] A number of SPR biosensors based on a gold/graphene have been designed and proposed to investigate the performance improvement numerically and experimentally.[33-37] *Wu* et al. have numerically studied a graphene-based SPR biosensor and obtained a sensitivity enhancement of 25% by coating graphene sheets on the SPR gold film with ten layers of graphene.[37] *Maharana* et al. have simulated the effect of graphene on the electric field enhancement and the performance of the SPR sensor, and improved the sensitivity by 22% over the bimetallic Ag-Au configuration.[38] *Meshginqalam* et al. have proposed an SPR biosensor based on a GO linking layer and showed that the optimized thickness of GO films (15 nm) deposited on the surface of the gold film leads to an enhancement of 23% compared to the control SPR sensor.[39] On the other hand, there are also many experimental reports, and most of them employed mono- or few layer of graphene oxide (GO) modifying the plasmonic interface to enhance the sensitivity. *Y Ryu* et al. obtained SPR sensitivity enhancement of 13% with GO modified SPR sensor. Furthermore, the simulated results indicate that the sensitivity could be further improved by GO stacking.[40] *YV Stebunov* et al. proposed a GO-SPR sensor, which shows a 20% sensitivity enhancement in the RI sensing part compared to the bare gold chip.[41] However, transferring mono- or few layer large-scaled graphene is a complicated process, and the sensitivity enhancement is also limited. Therefore, the GOSs are proposed to enhance the sensitivity in this work because of its much greater ability to enhance the electric field intensity and much larger surface area to capture the small biomolecules.

In this work, GOSs were experimentally introduced to the plasmonic interface by spin-coating onto the gold film to enhance the sensitivity of SPR sensors. Different from the reported work, the thickness of the GOSs overlayer was up to hundreds of nanometres, which still provides a significant improvement in sensitivity. The influence of GOSs overlayers with different thicknesses on the RI sensitivity was studied in detail. With the increase of the GOSs overlayer, the RI sensitivity increases first and then decreases. Based on the proposed sensor, a bio-experiment in detecting the bovine serum albumin was conducted, and the results demonstrated the advantage of GOSs materials for bio-molecules detection. To the best of our knowledge, this is the first report on using the spin-coating method to modify the GOSs in SPR-based sensors to enhance the RI sensitivity experimentally. The sensitivity enhancement method is much simpler to perform and has better effect than those using a complex nanostructure and nanoparticles or utilizing the graphene transfer method.

EXPERIMENTAL SECTION

Fabrication and characterization. Figure 1 shows the schematic diagram of the proposed GOSs-SPR sensor. The proposed SPR sensor is based on the conventional Kreschmann configuration, which consists of an SPR chip mounted on the top of a coupling prism. Firstly, a customized silica slide (Jiuyi Optics, Fuzhou, China) was treated by ultrasonic for 10 minutes, and then a 5 nm chromium layer for increasing the adhesion between the glass slide and the gold and a 50 nm gold layer were successively deposited onto the slide via vacuum evaporation. Finally, the prepared GOSs suspension was spin-coated onto the gold film at a spin rate of 3000 rpm for 180 seconds. The thickness of GOSs overlayer can be tailored by the number of times spin-coating. The GOSs (purchased from Nanoon Tec. Co., Ltd.) linked with carboxyl group were suspended in water with a concentration of 0.5 mg/ml. Before the spin-coating, the GOSs

suspensions were treated by ultrasonic for 30 minutes to ensure homogeneous dispersion of GOSs.

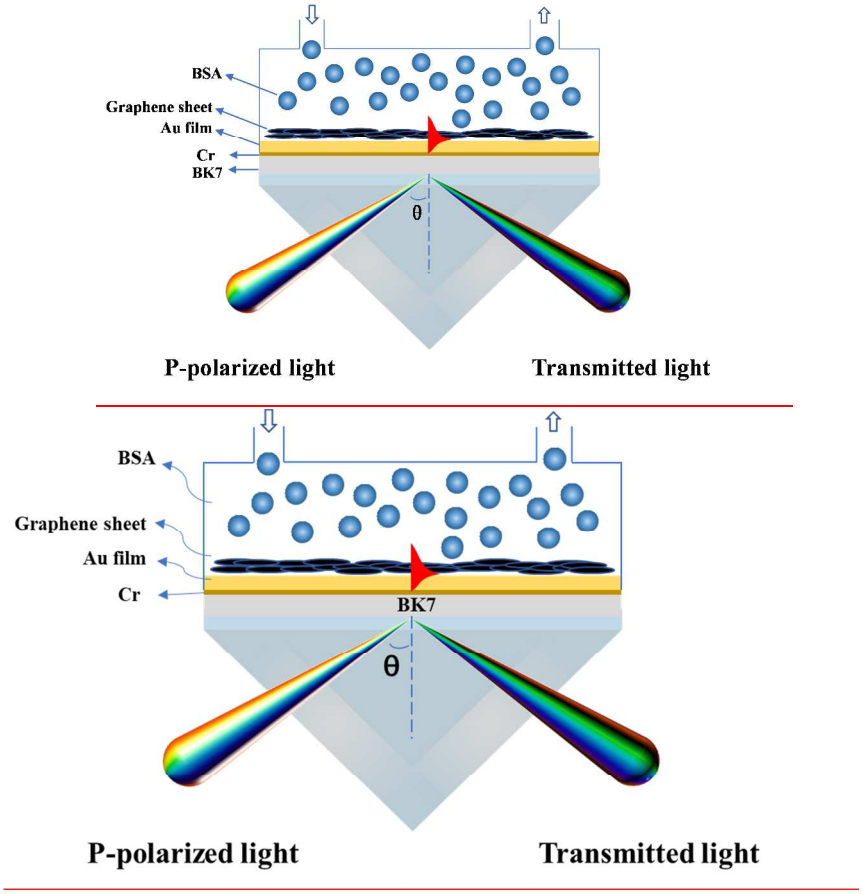

Figure 1. Schematic diagram of the proposed GOSs SPR sensor.

The absorbance of the GOSs suspension from 400 to 1100 nm was measured firstly. The measurement was conducted by coupling light from a tungsten−halogen lamp (AvaLight-HAL-(S)-Mini, China) to the sample cuvette and collecting the transmitted light with a spectrometer (AvaSpec-ULS2048XL, China). From the absorbance spectra of the GOSs suspension and the control sample (ethyl alcohol) as shown in Figure 2(a). It can be seen that there are two absorbance peaks at 434 nm and 981 nm, respectively. No absorption peaks can be found in the

range of 600 ~ 900 nm, which is the wavelength range of SPR occurring in the following experiments.

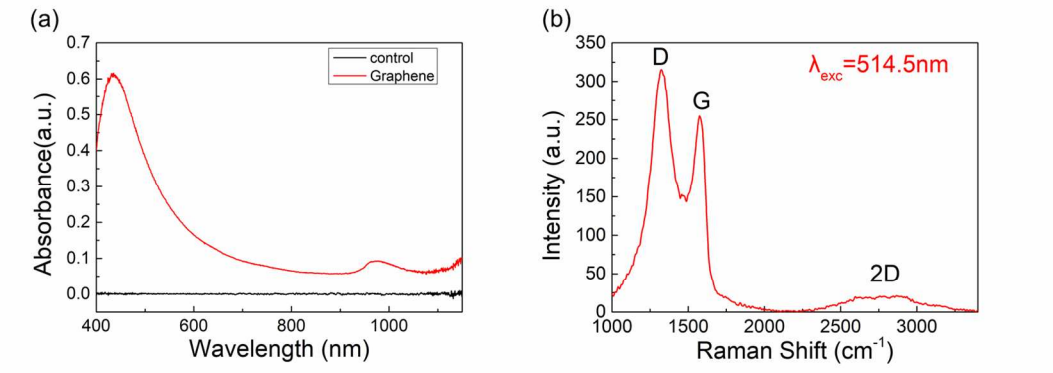

Figure 2. (a) Absorption spectrum of the prepared GOSs suspension. (b) Raman spectrum of the GOSs overlayer on the SPR sensor.

The Raman spectrum excited by a laser at wavelength 514.5 nm was measured with a Raman microscope (HORIBA JY LabRAM HR Evolution, France) and depicted in Figure 2(b). The D and G bands are located at 1330 cm^{-1} and 1575 cm^{-1}, respectively. By comparing the intensity ratios and peaks of the GOSs in Figure 2(b) with those in literature,[42] the GOSs overlayer coated on the gold film can be estimated to be multilayer.

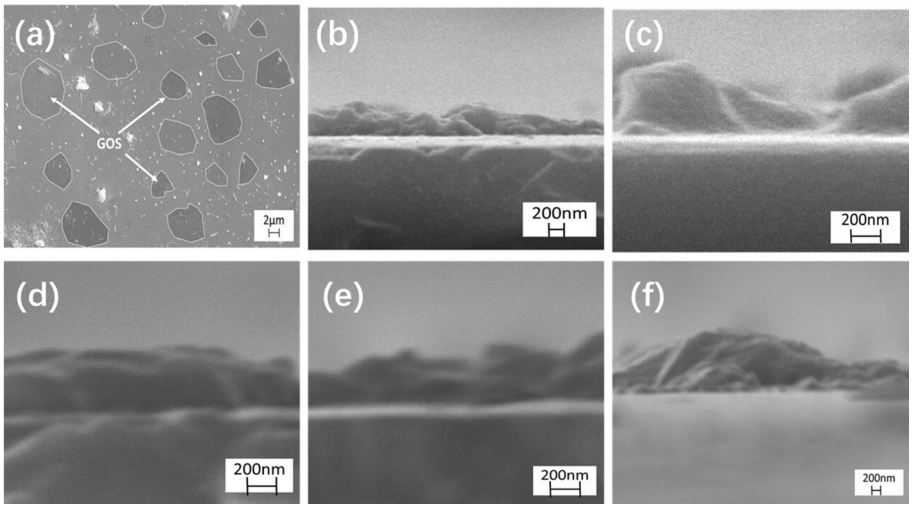

Figure 3. SEM photographs of GOSs-SPR senor surface (a). The GOSs cross section SEM images after spin-coating for (~~a~~b) one, (~~b~~c) two, (~~c~~d) three, (~~d~~e) four, (f) and five times.

To obtain the surface morphology and the thickness of the GOSs-SPR chips with different times of GOSs spin-coating, the surface and cross section of SPR sensors with GOSs were examined by a scanning electron microscopy (SEM, Zeiss SteREO Discovery V20, Germany) and shown in Figure 3(a) and Figure 3 (b)~(e), respectively. Before the SEM observation, a layer of gold was sputtered on the GOSs overlayer to increase its conductivity. The average thickness of the GOSs overlayer are measured to be 359.7, 409.8, 461.5, 535.4, and 758.6 nm for the GOSs-SPR chips with spin-coating times from one to five, respectively.

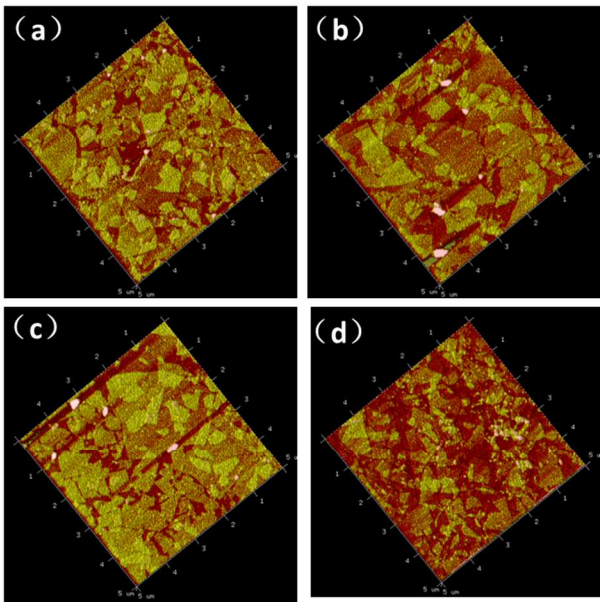

Figure 4. Three-dimensional AFM images for the surface of the sensors with different times spin-coating: (a) one; (b) two; (c) three; (d) four.

The atomic force microscopy (AFM) observation of the GOSs-SPR chips were performed using a Nanoscope IIIa controller (Veeco Instruments) in the tapping mode under ambient

conditions at a scanning rate of 1 line/s. As Figure 4 shows, the GOSs are randomly distributed on the surface of the gold film, and the GOSs become more concentrated with increasing spin-coating times. Actually, we measured the AFM image of five times spin-coating as well, but the probe of the AFM scratched the overlayer of the sensor because of the unduly thick overlayer of GOSs (estimated over 750 nm) and weak binding forces. Thus the AFM image of the sample with five times spin-coating could not be acquired.

Sensor performance measurement and discussion. The SPR was excited through a prism in Kretschmann configuration by mounting a GOSs-SPR chip on the top of a prism, and applying oil for index matching. The broadband signal light was first p-polarized and then coupled into the prism, and the SPR was excited by the evanescent wave at a certain wavelength, corresponding to a resonance dip formed in the reflected light, which was measured by the spectrometer. In the RI sensing experiments, solutions with different RIs were measured to evaluate the performance of the proposed GOSs-SPR and control Au-SPR chips, respectively. The solutions were obtained by mixing ethylene glycol and deionized water at a certain ratio, and their RIs were further measured by Abbe refractometer (Edmund NT52-975, Edmund Optics Co., Ltd.) at room temperature of 25℃. Figure 5 shows the transmittance spectra for the Au-SPR chip and GOSs-SPR chip with the RI of solution changing from 1.333 to 1.360 RIU. From each sub-figure, it is clearly seen from the spectra that the resonance dip shifts to the longer wavelength, and that the SPR dip width becomes wider and the depth of the dip becomes smaller along with the number of times spin-coating increase. As shown in Figure 5 (a)-(f), the total resonant wavelength shift increases from 61.16 to 73.59 nm and then decreases to 30.30 nm. The spectra for different GOSs spin-coating times at the environment RI of 1.333 RIU were picked out and plotted in Figure 6(a), which apparently shows that the resonance dip shifts to the longer wavelength.

Furthermore, the resonance wavelength and GOSs spin-coating times yield a linear equation of $y = 628.29 + 29.77x$, as shown in Figure 6(b). The fitting coefficient R^2 is 0.967.

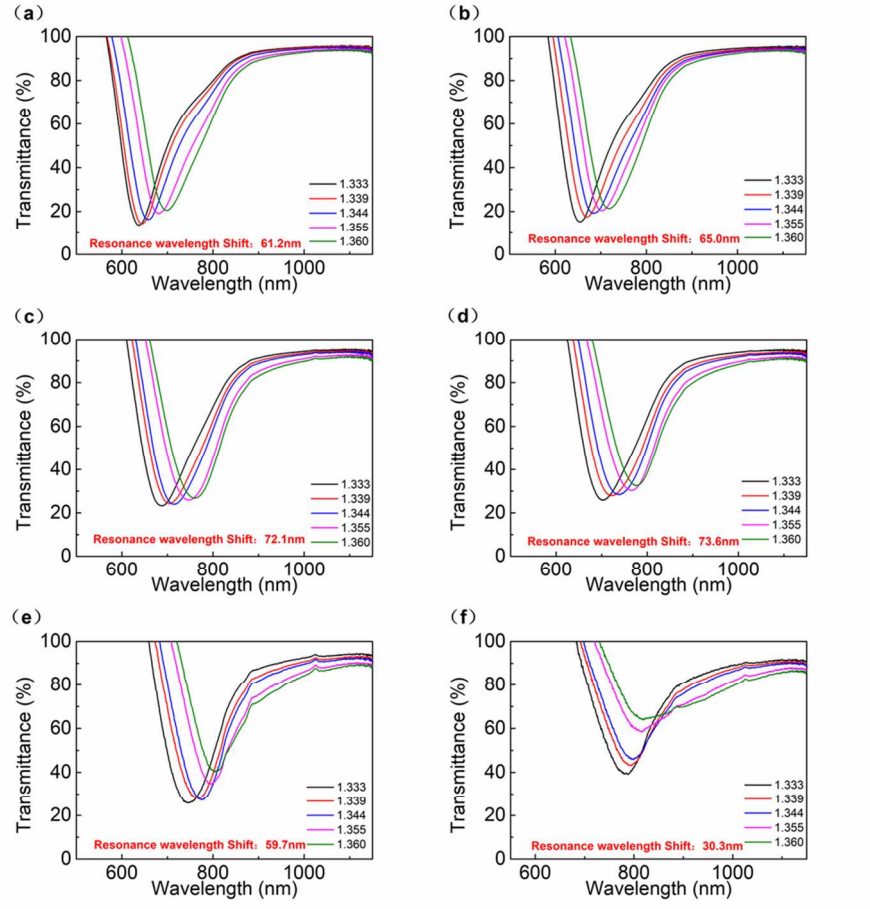

Figure 5. Transmittance spectra for GOSs-SPR sensor with different number of times spin-coating: (a) without coating; (b) one; (c) two; (d) three; (e) four; (f) five.

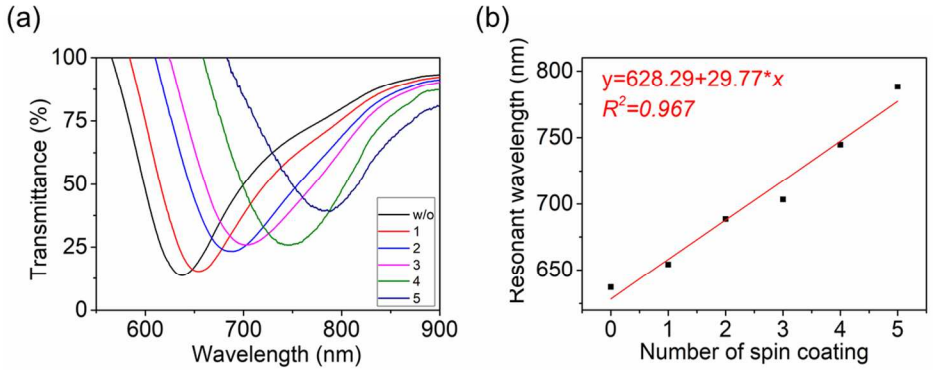

Figure 6. (a) spectra of GOSs-SPR sensors for different spin-coating times at the environment RI of 1.333 RIU; (b) relationship between the resonant wavelength and the number of GOSs spin-coating.

In order to describe the SPR sensor sensing performance, the sensitivity and figure of merit (FOM) were calculated, respectively. The sensitivity was defined as $S = \Delta\lambda/\Delta n$, where Δn represents the changed value of the sensed RI and $\Delta\lambda$ represents the corresponding wavelength shift of the resonance dips. The FOM was defined as FOM = S/FWHM, where the FWHM was the full width at half maximum of the resonance spectrum. Figure 7 illustrates the linear relation between the resonance wavelengths versus RIs variation. The slopes of fitting line represent the sensitivity of the sensor. The sensitivity for different times of GOSs spin-coating were further plotted in Figure 8(a). With the increase of the number of times spin-coating, the sensitivity firstly increased from 2257.9 nm/RIU to 2715.1 nm/RIU, and then decreased to 1194.7 nm/RIU. The highest sensitivity achieved by three times spin-coating is 2715.1 nm/RIU, and yields an enhancement of 20.2% than the case without a GOSs overlayer.

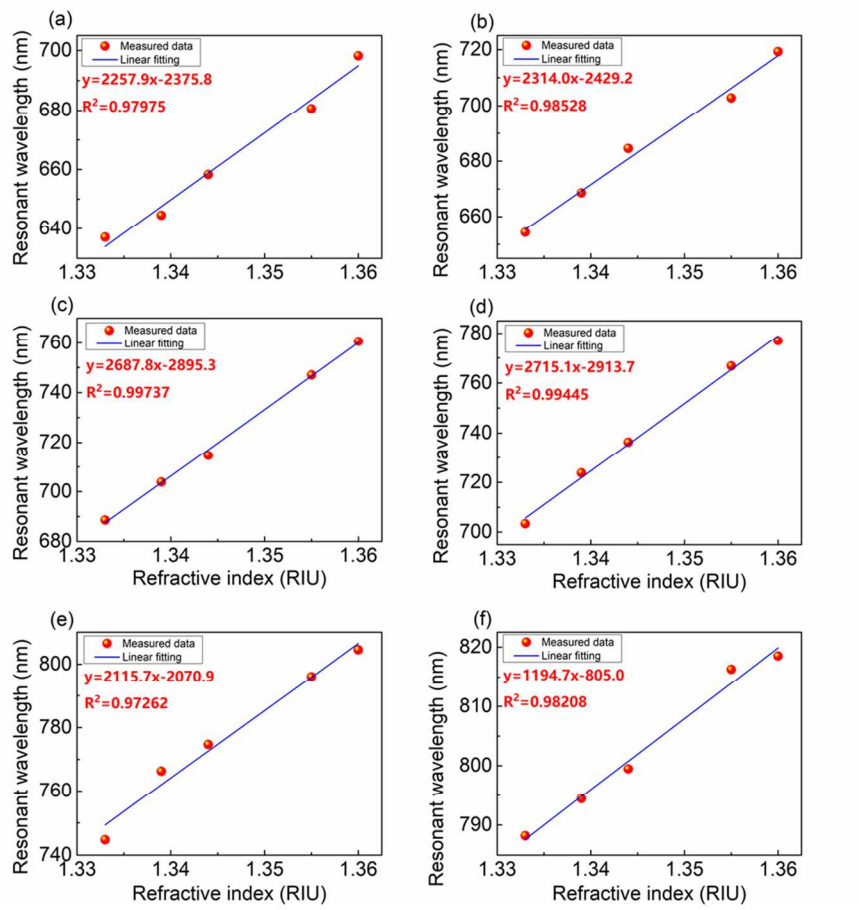

Figure 7. Experimental variation shifts in the resonance wavelength with RI under different number of times spin-coating: (a) without spin-coating; (b) one; (c) two; (d) three; (e) four; (f) five.

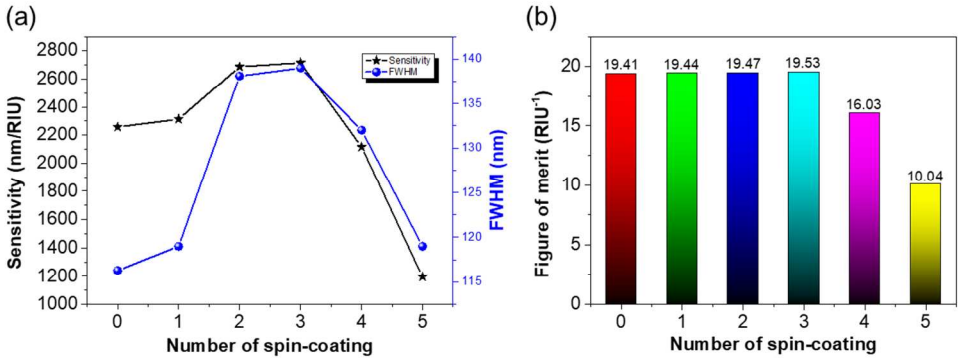

Figure 8. (a) Sensitivity, FWHM and (b) FOM for different times of spin-coating GOSs.

Figure 8(b) shows the FOMs variation as a function of the number of times of GOSs coating. Noted that, when calculating the FOM, the FWHM we measured is at the RI of 1.333. From Figure 8(b), it can be seen that the FOM first increases and then decreases with the increasing times of GOSs spin-coating. Firstly, the increasement of the sensitivity is greater than the FWHM, so the FOM increases. However, the excessive of GOSs (thicker than 461.5nm) stacked on the gold film and the rough surface of the overlayer can cause a strong absorption and scattering, which would broaden the SPR dip and result in the decrease of FOM. From Figure 8(b), it can be seen that the three times of GOSs spin-coating also has the highest FOM.

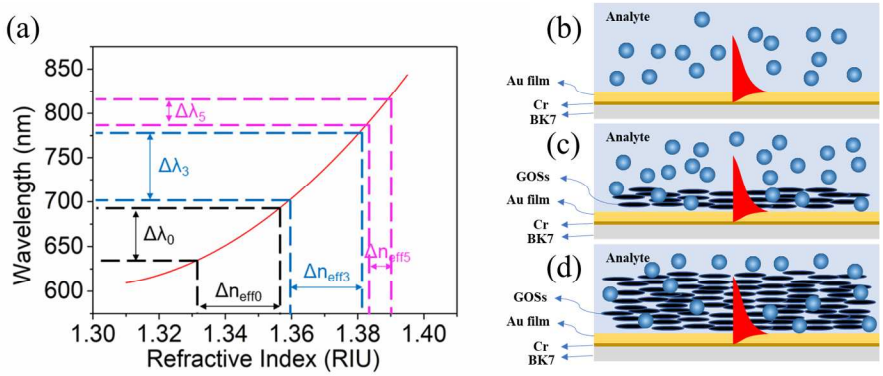

Figure 9. (a) Experimental variation of shift in the resonance wavelength with surrounding RI ranging from 1.31 to 1.395; Schematic diagram of the plasmonic interface of GOSs SPR sensor for: 0 (b), 3 (c), 5(d) times spin-coating.

To explain why the sensitivity first increases and then decreases, the GOSs and the analyte were treated as a hybrid sensing layer. The introduction of the GOSs will change the effective RI of the hybrid sensing layer and also the evanescent electric field distribution. We experimentally measured the SPR spectra of the sensor with the uncoated SPR sensor in the analyte of RI sensing ranging from 1.31 to 1.395 to analyze the influence of the effective RI on the sensitivity. It could be clearly seen from the Figure 9 that the sensitivity of the sensor, represented by the

slope of the curve, increases with the increased RI, which means the same RI increment in the high RI range will lead to a longer wavelength shift than that in the low RI range. After spin-coating the GOSs on the bare gold chip, the effective RI of the hybrid sensing layer changes. The corresponded effective RI can be described as $n_{eff} = f_{analyte} \times n_{analyte} + f_{GOS} \times n_{GOS}$, where $f_{analyte} = V_{analyte} / (V_{analyte} + V_{GOS})$ and $f_{GOS} = V_{GOS} / (V_{analyte} + V_{GOS})$ are the volume fractions of the analyte and GOSs, $V_{analyte}$ and V_{GOS} are the volumes of analyte and GOSs in the hybrid sensing layer, and $n_{analyte}$ and n_{GOS} are the RI of analyte and GOSs. One effect raised by introducing the GOSs is to change the fraction of analyte, $f_{analyte}$. The sensitivity of the sensor is calculated via $S = \Delta\lambda / \Delta n_{analyte}$, and the $\Delta n_{analyte}$ here is fixed at a value of 0.027 (1.333 to 1.360) in the experiment for different GOSs overlayer thickness. With the increase of GOSs overlayer thickness, f_{GOS} increases while $f_{analyte}$ decreases, which leads to the decrease of the effective RI increment, $\Delta n_{eff} = f_{analyte} \times \Delta n_{analyte}$. Although the Δn_{eff} decreased, the $\Delta\lambda$ may increase due to the large slope according to Figure 9(a). To be more intuitive, the wavelength shift for 0, 3, and 5 times GOSs spin-coating and the corresponding effective RI increments were sectioned via different color dash lines in Figure 9(a) and the schematic diagram of the plasmonic interface of GOSs SPR sensor were shown in Figure 9(b), (c) and (d). It can be clearly seen that although $\Delta n_{eff0} > \Delta n_{eff3}$, the corresponding $\Delta\lambda_3 > \Delta\lambda_0$, which means the sensitivity increases with the increasement of the thickness of the GOSs overlayer. However, this trend does not remain constant. Another effect of the introduced GOSs is to change the evanescent electric distribution, which in turn has an change on the decay length.[43] According to the fact that the decay length of the SPR evanescent field in the dielectric layer usually ranges from tens to hundreds nanometres,[44] the interaction between the evanescent field and analyte will be weaken with the thickness of GOSs overlayer increased to a certain value, which results that the sensitivity will come to a decreasing trend. For

example, the $\Delta\lambda_3$ is even smaller than the uncoated one ($\Delta\lambda_0$). Combining the two effects on the sensitivity brought by introducing the GOSs overlayer, the experimental result can be explained why the sensitivity first increases and then decreases.

To further confirm the sensitivity of the GOSs-SPR sensors in biological experiment, the phosphate buffer and BSA solutions (changing from 0 to 10 mg/ml with a step of 2.5 mg/ml) were flowed through the best GOSs-SPR sensor, i.e. the three times of GOSs spin-coated sensor. Figure 10(a) and (b) show the experimental variation of the resonance wavelength for conventional and the GOSs modified SPR sensors with different concentration of BSA solutions. And as shown in Figure 10(c) and (d), it can be clearly seen that GOSs-SPR sensor has an obvious improvement compared to the conventional Au-SPR sensor. The resonant wavelength shifts increase from 10.75 nm to 14.98 nm with an enhancement of 39.35%, which indicates that the modification of GOSs could improve the sensitivity even in a larger amplitude than that in bulky solutions and achieve a higher enhancement of FOM moreover.

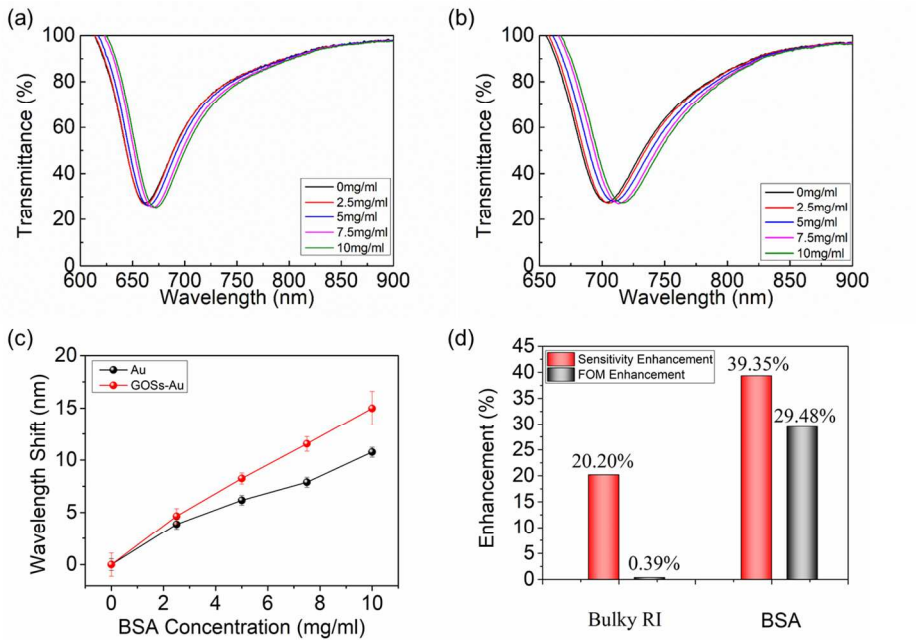

Figure 10. Response to the different concentration of BSA solutions without (a) and with three times (b) of GOSs spin-coating; (c) variation shifts in the resonance wavelength with BSA under three times spin-coating; (d) comparison of the enhancement in bulky RI solutions and BSA solutions.

Table 1 shows the comparison between the results from literature and our work, in terms of sensing target, the material scale, enhancement fold and the data acquisition approach. Noted that, among all the studies aiming at enhancing the SPR sensitivity with the graphene/graphene like materials, this work is the first time to apply GOSs with thickness up to hundreds of nanometres to enhance the sensitivity of SPR sensors and experimentally demonstrate competitive results in both bulky RI and BSA solutions.

Table 1. Comparison of SPR enhancement with various interface modification

Plamonic interface	Sensing Target	Material Scale	Enhancement	Theoretical/Experimental	Ref.
Au-Graphene	RI	10 layers	25%	Theoretical	37
	RI	0.34 nm	22%	theoretical	38
	RI	20 layers	50%	theoretical	45
	RI	0.34 nm	23%	theoretical	46
Au-GO	RI	15 nm	23%	theoretical	39
	RI	~10 nm	13%	experimental	40
	RI	14 nm	20%	experimental	41
	Goat anti-human IgG	Mono-/bilayer	56%	experimental	47
Au-GOSs	Anti-BSA	-	38%	experimental	35
	BSA	~461.5 nm	39%	experimental	This

CONCLUSIONS In summary, we have proposed and demonstrated a simple method to enhance the sensitivity of SPR sensor by spin-coating an overlayer of GOSs onto the gold film surface. The sensitivity related to the thickness of the GOSs overlayer can be tailored by the spin-coating times of GOSs suspension. With the increase of the number of times spin-coating, the sensitivity firstly increases from 2257.9 nm/RIU to 2715.1 nm/RIU, and then decreases to 1194.7 nm/RIU. The maximum sensitivity of 2715.1 nm/RIU can be achieved by spin-coating GOSs for three times, showing an enhancement of 20.2% compared to the uncoated case. Benefiting from the large surface area and abundant surface functional groups, the GOSs-SPR sensor shows a higher sensitivity enhancement (39.35%) in the detection of BSA molecules than that in bulky solution. Further research on binding interactions between the target molecules and the functional groups on the surface of the GOSs, will allow the proposed sensor to be a versatile platform for biochemical sensing applications.

AUTHOR INFORMATION

Xin Xiong and Yaofei Chen contributed equally to this work.

Corresponding Author

*E-mail: luoyunhan@jnu.edu.cn

ORCID

Yunhan Luo: 0000-0002-6587-832X

Yaofei Chen:0000-0002-7067-6562

Notes

The author declares no competing financial interest.

ACKNOWLEDGMENT

This work was partly supported by the National Natural Science Foundation of China (Nos. 61575084, 61475066, 61705087 and 61805108), the Natural Science Foundation of Guangdong Province (Nos. 2015A030313320, 2014A030313377 and 2016A030311019), the Science and Technology Projects of Guangdong Province (Nos. 2016B010111003 and 2016A010101017), the Science & Technology Project of Guangzhou (Nos. 201707010500, 201807010077, 201605030002 and 201704030105), the open project of Key Laboratory of Micro Opto-electro Mechanical System Technology, Tianjin University, Ministry of Education (MOMST 2016-6) and the Fundamental Research Funds for Central Universities (21618404 and 21617332).

REFERENCES

1. Homola, J., Present and future of surface plasmon resonance biosensors. *Anal Bioanal Chem* **2003,***377* (3), 528-39.
2. Lee, W.; Kim, D., Field-matter integral overlap to estimate the sensitivity of surface plasmon resonance biosensors. *JOSA A* **2012,***29* (7), 1367-1376.
3. Li, D.; Lu, H.; Qiu, W.; Dong, J.; Guan, H.; Zhu, W.; Yu, J.; Luo, Y.; Zhang, J.; Chen, Z., Molybdenum disulfide nanosheets deposited on polished optical fiber for humidity sensing and human breath monitoring. *Optics Express* **2017,***25* (23), 28407-28416.
4. Lu, Y.; Hao, C. J.; Wu, B. Q.; Huang, X. H.; Wen, W. Q.; Fu, X. Y.; Yao, J. Q., Grapefruit fiber filled with silver nanowires surface plasmon resonance sensor in aqueous environments. *Sensors (Basel)* **2012,***12* (9), 12016-25.
5. Lu, Z.; Chen, X.; Hu, W., A fluorescence aptasensor based on semiconductor quantum dots and MoS2 nanosheets for ochratoxin A detection. *Sensors and Actuators B: Chemical* **2017,***246*, 61-67.
6. Gnedenko, O. V.; Mezentsev, Y. V.; Molnar, A. A.; Lisitsa, A. V.; Ivanov, A. S.; Archakov, A. I., Highly sensitive detection of human cardiac myoglobin using a reverse sandwich immunoassay with a gold nanoparticle-enhanced surface plasmon resonance biosensor. *Anal Chim Acta* **2013,***759*, 105-9.
7. Guo, L.; Jackman, J. A.; Yang, H.-H.; Chen, P.; Cho, N.-J.; Kim, D.-H., Strategies for enhancing the sensitivity of plasmonic nanosensors. *Nano Today* **2015,***10* (2), 213-239.

8. Karlsson, R.; Stã¥Hlberg, R., Surface plasmon resonance detection and multispot sensing for direct monitoring of interactions involving low-molecular-weight analytes and for determination of low affinities. *Analytical Biochemistry* **1995,***228* (2), 274-280.
9. Shalabney, A.; Abdulhalim, I., Sensitivity - enhancement methods for surface plasmon sensors. *Laser & Photonics Reviews* **2011,***5* (4), 571-606.
10. Zeng, S.; Yu, X.; Law, W.-C.; Zhang, Y.; Hu, R.; Dinh, X.-Q.; Ho, H.-P.; Yong, K.-T., Size dependence of Au NP-enhanced surface plasmon resonance based on differential phase measurement. *Sensors and Actuators B: Chemical* **2013,***176*, 1128-1133.
11. Law, W. C.; Yong, K. T.; Baev, A.; Prasad, P. N., Sensitivity improved surface plasmon resonance biosensor for cancer biomarker detection based on plasmonic enhancement. *Acs Nano* **2011,***5* (6), 4858.
12. Chen, Y. Y.; Chang, H. T.; Shiang, Y. C.; Hung, Y. L.; Chiang, C. K.; Huang, C. C., Colorimetric Assay for Lead Ions Based on the Leaching of Gold Nanoparticles. *Analytical Chemistry* **2009,***81* (22), 9433-9439.
13. Roh, S.; Chung, T.; Lee, B., Overview of the Characteristics of Micro- and Nano-Structured Surface Plasmon Resonance Sensors. *Sensors* **2011,***11* (2), 1565.
14. Kabashin, A.; Evans, P.; Pastkovsky, S.; Hendren, W.; Wurtz, G.; Atkinson, R.; Pollard, R.; Podolskiy, V.; Zayats, A., Plasmonic nanorod metamaterials for biosensing. *Nature materials* **2009,***8* (11), 867.
15. Krasnykov, O.; Karabchevsky, A.; Shalabney, A.; Auslender, M.; Abdulhalim, I., Sensor with increased sensitivity based on enhanced optical transmission in the infrared. *Optics Communications* **2011,***284* (5), 1435-1438.
16. Slavík, R.; Homola, J., Ultrahigh resolution long range surface plasmon-based sensor. *Sensors & Actuators B Chemical* **2007,***123* (1), 10-12.
17. Nenninger, G. G.; Tobiška, P.; Homola, J.; Yee, S. S., Long-range surface plasmons for high-resolution surface plasmon resonance sensors. *Sensors & Actuators B Chemical* **2001,***74* (1), 145-151.
18. Singh, S.; Gupta, B. D., Simulation of a surface plasmon resonance-based fiber-optic sensor for gas sensing in visible range using films of nanocomposites. *Measurement Science and Technology* **2010,***21* (11), 115202.
19. Shalabaney, A.; Abdulhalim, I. S., Surface plasmon sensor with enhanced sensitivity using top nano dielectric layer. *Journal of Nanophotonics* **2009,***3* (3), 231-249.
20. Tabassum, R.; Gupta, B. D., Influence of oxide overlayer on the performance of a fiber optic SPR sensor with Al/Cu layers. *IEEE Journal of Selected Topics in Quantum Electronics* **2017,***23* (2), 81-88.
21. Wang, H.; Zhang, H.; Dong, J.; Hu, S.; Zhu, W.; Qiu, W.; Lu, H.; Yu, J.; Guan, H.; Gao, S.; Li, Z.; Liu, W.; He, M.; Zhang, J.; Chen, Z.; Luo, Y., Sensitivity-enhanced surface plasmon resonance sensor utilizing a tungsten disulfide (WS2) nanosheets overlayer. *Photonics Research* **2018,***6* (6), 485.
22. Yang, M.; Xiong, X.; He, R.; Luo, Y.; Tang, J.; Dong, J.; Lu, H.; Yu, J.; Guan, H.; Zhang, J.; Chen, Z.; Liu, M., Halloysite Nanotube-Modified Plasmonic Interface for Highly Sensitive Refractive Index Sensing. *ACS Appl Mater Interfaces* **2018,***10* (6), 5933-5940.
23. Ouyang, Q.; Zeng, S.; Jiang, L.; Hong, L.; Xu, G.; Dinh, X. Q.; Qian, J.; He, S.; Qu, J.; Coquet, P.; Yong, K. T., Sensitivity Enhancement of Transition Metal Dichalcogenides/Silicon Nanostructure-based Surface Plasmon Resonance Biosensor. *Sci Rep* **2016,***6*, 28190.
24. Maharana, P. K.; Jha, R.; Padhy, P., On the electric field enhancement and performance of

SPR gas sensor based on graphene for visible and near infrared. *Sensors & Actuators B Chemical* **2015,***207* (207), 117-122.
25. Chen, D.; Feng, H.; Li, J., Graphene oxide: preparation, functionalization, and electrochemical applications. *Chemical reviews* **2012,***112* (11), 6027-6053.
26. Novoselov, K. S.; Geim, A. K.; Morozov, S. V.; Jiang, D.; Zhang, Y.; Dubonos, S. V.; Grigorieva, I. V.; Firsov, A. A., Electric field effect in atomically thin carbon films. *science* **2004,***306* (5696), 666-669.
27. Bai, H.; Li, C.; Shi, G., Functional composite materials based on chemically converted graphene. *Advanced Materials* **2011,***23* (9), 1089-1115.
28. Chiu, N.-F.; Huang, T.-Y.; Lai, H.-C.; Liu, K.-C., Graphene oxide-based SPR biosensor chip for immunoassay applications. *Nanoscale research letters* **2014,***9* (1), 445.
29. Salah, N. H.; Jenkins, D.; Handy, R., Graphene and its Influence in the Improvement of Surface Plasmon Resonance (SPR) Based Sensors: a Review. *International Journal of Innovative Research in Advanced Engineering (IJIRAE)* **2014,***1* (10).
30. Eda, G.; Chhowalla, M., Chemically derived graphene oxide: towards large-area thin-film electronics and optoelectronics. *Adv Mater* **2010,***22* (22), 2392-415.
31. Johari, P.; Shenoy, V. B., Modulating optical properties of graphene oxide: role of prominent functional groups. *ACS nano* **2011,***5* (9), 7640-7647.
32. Cao, Y.; Lai, Z.; Feng, J.; Wu, P., Graphene oxide sheets covalently functionalized with block copolymers via click chemistry as reinforcing fillers. *Journal of Materials Chemistry* **2011,***21* (25), 9271-9278.
33. Chiu, N.-F.; Lin, T.-L.; Kuo, C.-T., Highly sensitive carboxyl-graphene oxide-based surface plasmon resonance immunosensor for the detection of lung cancer for cytokeratin 19 biomarker in human plasma. *Sensors and Actuators B: Chemical* **2018,***265*, 264-272.
34. Zeng, S.; Hu, S.; Xia, J.; Anderson, T.; Dinh, X.-Q.; Meng, X.-M.; Coquet, P.; Yong, K.-T., Graphene–MoS2 hybrid nanostructures enhanced surface plasmon resonance biosensors. *Sensors and Actuators B: Chemical* **2015,***207*, 801-810.
35. Chiu, N. F.; Huang, T. Y.; Lai, H. C.; Liu, K. C., Graphene oxide-based SPR biosensor chip for immunoassay applications. *Nanoscale Research Letters* **2014,***9* (1), 445-445.
36. Choi, S. H.; Kim, Y. L.; Byun, K. M., Graphene-on-silver substrates for sensitive surface plasmon resonance imaging biosensors. *Optics express* **2011,***19* (2), 458-466.
37. Wu, L.; Chu, H.; Koh, W.; Li, E., Highly sensitive graphene biosensors based on surface plasmon resonance. *Optics express* **2010,***18* (14), 14395-14400.
38. Maharana, P. K.; Padhy, P.; Jha, R., On the Field Enhancement and Performance of an Ultra-Stable SPR Biosensor Based on Graphene. *IEEE Photonics Technology Letters* **2013,***25* (22), 2156-2159.
39. Meshginqalam, B.; Ahmadi, M. T.; Ismail, R.; Sabatyan, A., Graphene/Graphene Oxide-Based Ultrasensitive Surface Plasmon Resonance Biosensor. *Plasmonics* **2016**, 1-7.
40. Ryu, Y.; Moon, S.; Oh, Y.; Kim, Y.; Lee, T.; Kim, D. H.; Kim, D., Effect of coupled graphene oxide on the sensitivity of surface plasmon resonance detection. *Applied Optics* **2014,***53* (7), 1419-26.
41. Stebunov, Y. V.; Aftenieva, O. A.; Arsenin, A. V.; Volkov, V. S., Highly Sensitive and Selective Sensor Chips with Graphene-Oxide Linking Layer. *Acs Applied Materials & Interfaces* **2015,***7* (39), 21727.
42. Kudin, K. N.; Ozbas, B.; Schniepp, H. C.; Prud'Homme, R. K.; Aksay, I. A.; Car, R., Raman spectra of graphite oxide and functionalized graphene sheets. *Nano letters* **2008,***8* (1), 36-

41.
43. Zeng, S.; Baillargeat, D.; Ho, H. P.; Yong, K. T., Nanomaterials enhanced surface plasmon resonance for biological and chemical sensing applications. *Chemical Society Reviews* **2014,***43* (10), 3426.
44. Homola, J., Present and future of surface plasmon resonance biosensors. *Analytical and bioanalytical chemistry* **2003,***377* (3), 528-539.
45. Fu, H.; Zhang, S.; Chen, H.; Weng, J., Graphene Enhances the Sensitivity of Fiber-Optic Surface Plasmon Resonance Biosensor. *IEEE Sensors Journal* **2015,***15* (10), 5478-5482.
46. Simsek, E., Improving Tuning Range and Sensitivity of Localized SPR Sensors With Graphene. *IEEE Photonics Technology Letters* **2013,***25* (9), 867-870.
47. Zhang, H.; Sun, Y.; Gao, S.; Zhang, J.; Zhang, H.; Song, D., A novel graphene oxide-based surface plasmon resonance biosensor for immunoassay. *Small* **2013,***9* (15), 2537-2540.